Fresh, freeze-dried or cell wall samples: Which is the most appropriate to determine chemical, structural and rheological variations during apple processing using ATR-FTIR spectroscopy?

Weijie Lan, Catherine M.G.C. Renard, Benoit Jaillais, Alexandre Leca, Sylvie Bureau

Fresh, Freeze-dried or Cell Wall Samples: Which is the Most Appropriate to Determine Chemical, Structural and Rheological Variations During Apple Processing Using ATR-FTIR Spectroscopy?

Weijie Lan[a], Catherine M.G.C. Renard[a,c], Benoit Jaillais[b], Alexandre Leca[a], Sylvie Bureau[a]*

[a,] UMR SQPOV, INRAE, Avignon University, F-84000 Avignon, France.

[b,] Stat SC, INRAE, ONIRIS, F-44300 Nantes, France.

[c,] TRANSFORM, INRAE, F-44300 Nantes, France.

Corresponding authors*

Sylvie Bureau (E-mail: sylvie.bureau@inrae.fr).

INRAE, UMR408 SQPOV « Sécurité et Qualité des Produits d'Origine Végétale »

228 route de l'Aérodrome

CS 40509

F-84914 Avignon cedex 9

Tel: +33 432722509

Other authors

Catherine M.G.C Renard: catherine.renard@inrae.fr

Benoit Jaillais: benoit.jaillais@inrae.fr

Alexandre Leca: alexandre.leca@inrae.fr

Weijie Lan: weijie.lan@inrae.fr

Highlights:

Proposition of puree sample preparation according to the expected quality traits.

Similar spectral fingerprints due to processing in fresh and freeze-dried samples.

ATR-FTIR on fresh purees could predict particle size and volume affecting texture.

ATR-FTIR on freeze-dried purees could assess viscosity and viscoelasticity.

ATR-FTIR on cell walls could highlight their changes during processing.

Abstract

Attenuated total reflectance Fourier transform spectroscopy (ATR-FTIR) was applied on fresh (NF), freeze-dried (FD) and cell wall materials (AIS) of raw and processed apples. These samples prepared from 36 apple sets and the corresponding 72 purees, issued from different varieties, agricultural practices, storage periods and processing conditions, were used to build models including exploratory analysis, supervised classification and multivariate calibration. Fresh and freeze-dried samples presented similar fingerprint spectral variations due to processing. ATR-FTIR directly on fresh purees satisfactorily predicted textural properties such as particle average size and volume (RPD> 3.0), while freeze-drying improved assessment of chemical (RPD> 3.2) and rheological (RPD> 3.1) parameters using partial least-squares regression. The assessment of texture and macrocomponents of purees can be obtained with a limited sample preparation. For research applications because of a need of sample preparation, changes of cell wall composition during fruit processing could be assessed in relationship with pectin degradation.

Keywords: *Malus domestica* Borkh., Mid infrared spectroscopy, apple processing, Partial Least-Squares Regression (PLSR), discrimination

1. Introduction

Sample preparation is a key point for quality of analytical data. Infrared spectroscopy (near or mid-infrared), because of its integrative nature, is one of the main candidates for a rapid qualification of agricultural commodities and processed food, especially in the view of process analytical technology (PAT). Advanced techniques based on infrared spectroscopy offer the advantages of a minimal sample preparation and a rapid data acquisition. However, this questions the balance between data intensity and required sample preparation hence man-power: are the data acquired on "raw" samples sufficient for process monitoring, quality control or process comprehension? A specific point is also that foods are frequently highly hydrated and not stable, so that appropriate steps must be taken to preserve samples for later quality control. As the time consumption and cost of sample preparation are generally barriers to a rapid and precise determination by spectroscopy, knowing the most efficient sample pretreatments could contribute to improve analytical results as well as to provide informative options at both, laboratory and industrial scales.

Different methods for the reference data acquisition such as HPLC, GC-MS or NMR (Bureau et al., 2013), types of spectroscopy or related hyperspectral images (NIR, MIR, Raman) (Baranska, Schütze, & Schulz, 2006) and modeling algorithms (Van Boekel, 2008) have been intensively compared on fruits. It seems also crucial to compare and determine the optimal sample form (fresh, freeze-dried or cell wall extracts) and the associated changes occurring during fruit processing, notably using infrared spectroscopy which has the potential to be applied both, on-line and off-line.

Direct ATR-FTIR estimations on fruit fresh homogenates have obtained good results to predict soluble solids content, dry matter content, titratable acidity, some individual sugars and organic acids (Bureau, Ścibisz, Le Bourvellec, & Renard, 2012; Ayvaz et al., 2016). As infrared spectroscopy is extremely sensitive to changes of hydrogen bonding (Jackson & Mantsch, 1995), the main drawback of spectral measurements is the low sensitivity and limited specific signals of chemical compositions under strong water interactions in fresh fruit suspensions, such as citric

acid in apples (Bureau, Ścibisz, Le Bourvellec, & Renard, 2012), lycopene and β-carotene in tomato (Baranska, Schütze, & Schulz, 2006). Moreover, classical measurements of rheological properties and particle size distribution of fruit products require costly rheometer, particle sizing equipment and experienced staffs. Therefore, one of the challenging works is to investigate the possibility of ATR-FTIR to estimate the specific rheological modifications (viscosity and viscoelastic parameters) and then to monitor textural changes (particle size and volume) for both, accurate determinations in scientific research or rapid and direct assessment in industrial processing.

Much more information can be extracted from dry food commodities, such as the structural changes of cereals (Georget & Belton, 2006), micronutrients in fruits (Lu et al., 2011) and even cell wall content variations (Canteri, Renard, Le Bourvellec, & Bureau, 2019). To overcome the limitations observed on highly hydrated products, such as fruits, drying methods with as limited as possible alteration of composition and structure are needed. Thus, freeze-drying prevents evolution of samples under the action of endogenous enzymes (notably oxidation and hydrolysis). It also carries out a concentration due to water elimination, so that specific components present in low concentrations can have significant spectral absorptions. But freeze-drying is expensive and time-consuming, needing at least 24-48 hours. It allowed to obtain similar predictions of chemical compositions than those in fresh samples (de Oliveira, de Castilhos, Renard, & Bureau, 2014; Oliveira-Folador et al., 2018). Few detailed studies compared the differences and limitations of ATR-FTIR fingerprint regions on fresh and corresponding freeze-dried plant leaves (Durak & Depciuch, 2020).

ATR-FTIR applications to assess fruit textural properties (mainly focus on cell wall compositions) are always performed on their cell wall materials (AIS) (Canteri, Renard, Le Bourvellec, & Bureau, 2019; □zymanska-Chargot, Chylinska, Kruk, & Zdunek, 2015). However, extracting the cell wall requires a large consumption of chemical solvents if starting from fresh samples (up to 1 L ethanol and 0.4 L acetone/ 1.0 - 1.5 g cell wall). The accelerated or pressurized solvent extractors (ASE, PSE)

can allow multiplexing and thus a faster and less solvent-consuming cell wall preparation, but only from already freeze-dried samples. After removing all soluble components (mainly sugars and acids), specific signals related to pectins, cellulose and hemicelluloses have proven to be useful for the fast evaluation of cell wall polysaccharides during fruit growth and subsequent storage (Szymanska-Chargot, Chylinska, Kruk, & Zdunek, 2015). Although some cell wall modifications in plants (Femenia, García-Pascual, Simal, & Rosselló, 2003) and fruits (Cardoso et al., 2009) under heating and dehydration have been investigated by ATR-FTIR. However, for fruit processed purees, little work has been done on ATR-FTIR to detect their cell wall changes during processing and monitor rheological and mechanical properties (Ferreira, Barros, Coimbra, & Delgadillo, 2001).

In this study, ATR-FTIR spectroscopy was applied on the corresponding raw apples and processed purees. Spectra were acquired on different kinds of homogeneous samples such as fresh (NF for non-freeze-dried), freeze-dried (FD) and cell wall extracts (AIS for alcohol insoluble solids) in order to: i) evaluate how much sample preparation improved the prediction of chemical, textural and rheological characteristics of purees (number of quality traits and their precision) and ii) identify signals specific of the variations which occur during apple processing.

2. Materials and methods

2.1 Plant Material

Apples of two cultivars: 'Golden Delicious' (GD) and 'Granny Smith' (GS) were harvested at commercial maturity in 2017 in an experimental orchard named La Pugère (Mallemort, Bouches-du-Rhône, France). Standard commercial fruit thinning practices (Th+ to 50 to 100 fruits/tree) and no thinning (Th- to 150-200 fruits/tree) were compared during the ripening of 'Golden Delicious'. The three obtained apple groups (Th+ GD, Th- GD and GS) were stored in a cold chamber at 4°C and at around 90% of humidity during one, three and six months (respectively T1, T3 and T6), except the first batch (T0) were analyzed and processed the day after harvest without any storage time.

Each apple batch (T0, T1, T3 and T6) was divided into two subsets (**Figure 1**):

i) the first subset was dedicated to apples characterization: 3 replicates of 10 apples were selected and separated into two aggregate samples as described by Bureau (Bureau, Ścibisz, Le Bourvellec, & Renard, 2012). One sample corresponding to the NF sample was stored at -80°C and then homogenized at 11000 rpm with an Ultraturrax T-25 (IKA, Labortechnik, GmbH, Staufen, Germany) after 1.5 h of thawing at 22.5 °C for biochemical and spectral characterizations. The other sample corresponding to the freeze-dried (FD) was used to extract cell wall materials (AIS). Finally, 36 NF, FD and AIS samples (3 apple groups × 4 storage times × 3 biological replicates) of raw apple fruits were obtained.

ii) the second sub-set was dedicated to puree processing: 3 replicates of apples (4 kg each) were used to produce three puree lots. After sorting and washing, apples were cored and cut in 8 portions, then processed in a multi-functional processing system (Roboqbo, Qb8-3, Bentivoglio, Italy). Half of the each puree (2 kg) was refined with a 0.5 mm (Ra) sieve (Robot Coupe C80 automatic refiner, Robot Coupe SNC, Vincennes, France) whereas the other half was not refined (NR). Finally, fresh puree samples (NF) were conditioned in two hermetically sealing cans: one was cooled at room temperature (22.5 °C) before the next-day measurements of rheological, textual and some chemical (soluble solids and titratable acidity) properties, while the other was freeze-dried (FD) and stored at -20 °C for AIS extraction. Thus, in total 72 NF, FD and AIS samples of purees were prepared and characterized, corresponding to 3 apple groups × 4 storage times × 2 refining levels × 3 biological replicates.

2.2 Biochemical Analyses

Soluble solids content (SSC) was determined with a digital refractometer (PR-101 ATAGO, Norfolk, VA, USA) and expressed in °Brix at 20°C. Titratable acidity (TA) was determined by titration up to pH 8.1 with 0.1 mol/L NaOH and expressed in mmol H^+/kg of fresh weight (FW) using an autotitrator (Methrom, Herisau, Switzerland). Sugars (glucose, fructose and sucrose) and malic acid were

quantified using an enzymatic method with kits for food analysis (Sigma-Aldrich, Deisenhofen, Germany) and expressed in g/kg FW. These measurements were performed with a SAFAS flx-Xenius XM spectrofluorimeter (SAFAS, Monaco). The dry matter content (DMC) was estimated with the weight of freeze-dried samples upon reaching a constant weight (freeze-dryer, 5 days). Cell wall materials (AIS) were isolated using the method proposed by Renard (Renard, 2005). and the cell wall contents (AIS contents) were expressed in both, fresh weight (FW) and dry matter weight (DW). Three biological replicates were characterized for each biochemical trait and each sample.

2.3 Rheological Analyses

The puree rheological measurements consisted in one rotational (flow curve) and two oscillatory (amplitude and frequency sweeps) tests, carried out using a Physica MCR-301 controlled stress rheometer (Anton Paar, Graz, Austria) at 22.5 °C. 50 mL of each puree sample was placed in a C-CC27 with an inner radius of 14.46 mm measuring cup (Anton Paar, Graz, Austria). All tests were performed by a six blade vane geometry FL 100/6W with a radius of 11 mm (Anton Paar, Graz, Austria). The flow curves were performed after a pre-shearing period of 1 minute at 50/s followed by 5 minutes at rest. The viscosity was then measured at a controlled shear rate range of [10; 250]/s on a logarithmic ramp, at a rate of 1 point every 15 seconds. The values of the viscosity at 50/s and 100/s (η_{50} and η_{100} respectively) were kept as indicators of the sensorial puree texture (Engelen & de Wijk, 2012; Espinosa-Muñoz et al. 2012) during consumption. Amplitude Sweep (AS) tests were performed at an angular frequency of 10 rad./s in the deformation range of [0.01; 100] %, in order to determine the linear viscoelastic range of the purees and the yield stress, defined as the crossing point between the storage modulus (AS-G') and the loss modulus (AS-G'') curves. Frequency Sweep (FS) measurements were operated within the linear viscoelastic region as determined by the AS test (0.05%) in the angular frequency range of [0.1; 100] rad./s. For means of comparison the storage and loss moduli (FS-G' and FS-G'') were taken at 1 rad./s to evaluate the viscoelastic

properties of the studied purees. Puree samples were diluted in distilled water to separate particles and stained with calcofluor white at 0.1 g/L and highlighted with a 365 nm UV lamp (Soukup, 2014). A high-resolution digital video camera (Baumer VCXU31C, Baumer SAS, France) with a macro lens (VSTech 0513, VS Technology Corporation, Japan.) was used to visualize the distribution and dispersion of puree particles. The particle sizes averaged over volume d(4:3) (de Brouckere mean) and over surface area d(3:2) (Sauter mean) were measured with a laser granulometer (Rawle, 2003) (Mastersizer 2000, Malvern Instruments, Malvern, UK).

2.4 ATR-FTIR spectrum acquisition

ATR-FTIR spectra were collected at room temperature using a Tensor 27 FTIR spectrometer (Bruker Optics, Wissembourg, France) equipped with a horizontal attenuated total reflectance (ATR) sampling accessory and a deuterated triglycine sulphate (DTGS) detector. Three replications of spectral measurement were performed on all raw and processed apples for fresh (NF for non freeze-dried), freeze-dried (FD) and cell wall (AIS) samples. The spectra of all samples were acquired in random order. The instrument adjustment and spectral acquisition were controlled by OPUS software Version 5.0 (Bruker Optics®). The spectra of raw and processed apples were acquired using two different crystals. A big zinc selenide (ATR-ZnSe) crystal with dimensions of 6 cm x 1 cm and six internal reflections was used for fresh samples (apple homogenates and purees) containing water. For the freeze-dried and cell wall samples, a small crystal was used characterized by a single-reflectance horizontal ATR-Diamond Cell (Golden Gate Bruker Optics) equipped with a press tip flap system to press sample on the crystal always in the same way. Spectra (32 scans for ATR-ZnSe and 16 scans for ATR-Diamond) were collected from 4000 cm^{-1} to 650 cm^{-1} and were corrected against the background spectrum of air.

2.5 Statistical Analyses and Chemometrics

After ensuring normal distribution with a Shapiro-Wilk test (α=0.05), the reference data were presented as mean values and the data dispersion within our

experimental dataset expressed as standard deviation values (SD). Analysis of variance (ANOVA) was carried out to determine the significant differences due to the controlled factors (thinning, storage and puree mechanical refining) on both apples (**Table S-1**) and purees of each variety (**Table S-2 and Table S-3**) using XLSTAT (version 2018.5.52037, Addtionsoft SARL, Paris, France) data analysis toolbox.

Spectral pre-processing and multivariate data analysis were performed with Matlab 7.5 (Mathworks Inc. Natick, MA) software using the SAISIR package (Bertrand & Cordella, 2008). The absorption band between 2400-2300 cm^{-1}, due to carbon dioxide, was discarded prior to the calculation. All FT-IR data were pre-processed with baseline correction, standard normal variate (SNV) and a derivative transform calculation Savitzky–Golay method, gap size = 11, 21, 31) of first or second order. After pretests of these pre-processing treatments applied on several different spectral regions, the best results of prediction and discrimination were obtained on the range 1800-900 cm^{-1}, which has been already highlighted (Bureau et al., 2009). Particularly, Principal Component Analysis (PCA) and Factorial Discriminant Analysis (FDA) were applied on SNV pre-treated spectra (in **Part 3.1** and **Part 3.2**). The specificity and sensitivity values of FDA discriminations were calculated by the already reported method of Nargis (Nargis et al., 2019), in order to better evaluate sample differentation. For PLS (Partial least square) modelling (in **Part 3.3**), the baseline correction coupled with SNV pre-processing had the best performances to correct multiplicative interferences and variations in baseline shift, and reached the best prediction results.

Leave-one-out PLS models were developed using spectra of fresh (NF), freeze-dried (FD) and AIS of puree samples, for which the three spectral matrices (NF, FD and AIS) corresponded to the same reference dataset. A total number of 72 averaged spectra for each puree form (NF, FD and AIS) corresponding to 3 apple groups (GS, GD Th+ and GD Th-) × 4 storage times × 2 puree refining modalities × 3 biological replicates was used as modelling dataset. PLS model performance was assessed using the determination coefficient of cross-validation (R_{cv}^2), the

root-mean-square error of cross-validation (RMSECv), the number of latent variables (LVs), the ratio of the standard deviation values (RPD) and the linkable spectral regions (**Tables 1 and 2**). The linearity correlation plots between measured and predicted values of all PLS models were showed in supplementary materials (**Figure S-5 and Figure S-6**).

3. Results and discussions

3.1 Spectral characterization of NF (non-freeze-dried) apple purees

PCA and FDA applied on the spectra of NF puree samples successfully allowed to detect puree differences coming from the raw apple variabilities (cultivar, fruit thinning and storage period) **(Figure 2)**. They also highlighted the modifications of puree structure by the mechanical refining over several months of apple storage **(Figure 3)**.

In **Figure 2**, the first principal component (PC1) clearly discriminated the two varieties ('Golden Delicious' and 'Granny Smith') and thinning practices for Golden delicious (Th- and Th+), in relation with the fructose variation followed at 1061 cm^{-1} (Bureau, Cozzolino, & Clark, 2019). Moreover, the peak at 1022 cm^{-1}, reported as a peak specific to sucrose in apple juices (Leopold, Leopold, Diehl, & Socaciu, 2011), appeared to be the main contributor of the second principal component (PC2), which distinguished the storage times. Along the PC2 axis, the discrimination of storage durations from T0 at the top to T6 at the bottom was in relation with the decrease of sucrose (1022 cm^{-1}) and the increase of fructose (1065 cm^{-1}) in purees, in accordance with the reference chemical dataset **(Table S-2)**. Consequently, factors such as cultivar, thinning practice and storage duration affecting raw apple characteristics induced changes in the corresponding purees after processing. ATR-FTIR applied directly on processed purees could then be useful for traceability of these effects impacting raw fruits based on the specific C-C and C-O-C bonds of carbohydrates, such as 1022 cm^{-1}, 1061 cm^{-1}, 1065 cm^{-1}.

According to the reference data **(Table S-2)** and their PCA results **(Figure S-1)**, the mechanical refining resulted a clear reduction of cell wall contents (AIS in DW and FW), viscosity (η_{50} and η_{100}), viscoelasticity (yield stress, G' and G'' in both oscillatory tests), particle size (d(4:3) and d(3:2)) in T0 purees prepared with apples at harvest (T0). However, gradually over apple storage, less differences were detected between the non-refined (NR) and refined (Ra) purees. The non-refined (NR) 'Golden Delicious' and 'Granny Smith' purees were characterized by large apple particles and only few small separated cells at the beginning of cold storage (T0) **(Figure 3a)**. The refining treatments mainly led to lower particle size by removing the big puree particles **(Figure 3a)**. However, at the end of storage (T6), both non-refined (NR) and refined (Ra) purees were mostly composed of single cells and no clear difference was observed between them **(Figure 3d)**. This similar structure of NR and Ra purees at T6 could be due to an increase in cell separability linked to a decrease of the intermolecular bonding between cell wall polymers and a notable increase of pectin solubility during apple storage (Varela, Salvador, & Fiszman, 2007).

FDA performed on the spectra of all NR and Ra purees (NF samples) at each apple storage time gave highly consistent observations with the reference data and macroscopic images showed above **(Figure 3)**. According to the third factorial components (F3) (F1 and F2 for cultivar and thinning discriminations, **Figure S-2**), the two puree refining levels were well separated at T0, then appeared progressively overlapped at T3 and T6 **(Figure 3)**. Especially along the F3 axis, at T0, intensive spectral variations were related to the decrease of soluble organic acids (1718 cm^{-1} and 1709 cm^{-1}), soluble polysaccharides, pectins and absorbed water (1740 cm^{-1}, 1695 cm^{-1}, 1682 cm^{-1}, 1668 cm^{-1}, 1655 cm^{-1} and 1468 cm^{-1}) between the two refining conditions **(Figure S-3)**. Although the peaks of carbohydrates at 1019 cm^{-1} and 1049 cm^{-1} (glucose/fructose) and 1155 cm^{-1} (the glycosidic linkage) are known to successfully monitor the consistency of tomato juice (Ayvaz et al., 2016), the region between 1750 and 1450 cm^{-1} highly contributed to the discrimination of apple purees according to their particle size and their rheological behavior after mechanical

refining treatments. These differences between tomato and apple might be due to the nature of the datasets and in particular the impact of post-harvest storage on chemical compositions (sugars and acids) and textural properties (pectins degradations) as confounding factors in this apple processing experiment.

3.2 Spectral evaluation of the link between fresh and processed apples

FDA results showed a good ability to discriminate puree processing changes (**Figure 4**) and cultivar differences **(Figure S-4)**, according to the first two discriminant factors (F1 and F2). Whatever the sample preparation (NF, FD and AIS), a clear separation was observed between raw apples (homogenates) and processed purees **(Figures 4 a, c, e)**. The changes occurring during processing between raw (homogenates) and processed (purees) products were illustrated on the first factorial axis (F1) for the NF samples (with 97.2% specificity and 98.6% sensitivity) and AIS materials (100% specificity and sensitivity), and on the second factorial axis (F2) for FD samples (100% specificity and sensitivity).

Combining the main discriminant coefficients of the FDA models separating raw and processed materials (F2 for NF and FD samples, F1 for AIS samples) **(Figures 4 b, d, f)** and using the absorption band assignments described in literature, allowed to identify phenomena occurring during apple processing. In both NF and FD samples, highly consistent variations of spectral intensity were commonly found between 1800 and 1500 cm^{-1}, this region giving overlapped information related to pectins, proteins, phenolics and absorbed water (Kačuráková et al., 1999), detailed in the following section:

- The increase of the bands at 1750 cm^{-1} in NF **(Figure 4b)**, 1788 cm^{-1} and 949 cm^{-1} in FD **(Figure 4d)** were specific of C=O, C-O and C-C stretching vibrations of carboxylic acids and polysaccharides (Canteri, Renard, Le Bourvellec, & Bureau, 2019; Kyomugasho et al., 2015). These observations were in accordance with the increase of soluble fiber fractions and total polysaccharide contents after apple cooking (Colin-Henrion, Mehinagic, Renard, Richomme, & Jourjon, 2009).

- The bands at 1610-1620 cm^{-1} (1614 cm^{-1} in NF; 1618 cm^{-1} in FD) have been

reported to correspond to the vibration of C=O from protein or pectic acid ester (Abidi, Cabrales, & Haigler, 2014). These peaks were consistent with the aforementioned pectic absorption peaks (1750 cm^{-1} and 1788 cm^{-1}), in accordance with the increase of pectin content in purees. In the same way, this absorbance displays the same variations in a simplified experiment of apple cell wall (mainly soluble pectins) submitted to similar puree processing conditions (100°C for 20 min at pH 3.0) (Liu, 2019). In addition, the negligible concentration of proteins in fresh and processed apples (0.17-0.57 g/100 g FW) limited the hypothesis concerning the protein change during apple processing (U.S. Department of Agriculture, Agricultural Research Service , 2019).

- the strong decrease of bands near 1630 cm^{-1} and 1560 cm^{-1} could be attributed to the degradation of phenolic compounds during processing. These bands have been already identified to quantify the polyphenol contents in freeze-dried apples (Bureau, Ścibisz, Le Bourvellec, & Renard, 2012).

- the specific bands of soluble acids (1712 cm^{-1} in NF, 1718 cm^{-1} in FD) (Clark, 2016) and of sugars (fructose at 1084 cm^{-1} and 1061 cm^{-1}; sucrose at 1113 cm^{-1}) (Bureau, Cozzolino, & Clark, 2019), which have been validated with standard chemicals in ATR-FTIR, could partially contribute to the dynamics of puree changes. These spectral variations relating the decreases of acid contents and increases of fructose at 1712 cm^{-1} were also in line with the results of chemical measurements **(Table S1 and Table S2).**

In cell wall materials (AIS), two negative peaks at 1100 cm^{-1} and 984 cm^{-1} **(Figure 4f)**, could be attributed to the solubilization of the cell wall pectins after thermal processing (Coimbra, Barros, Barros, Rutledge, & Delgadillo, 1998; Kacurakova, Capek, Sasinkova, Wellner, & Ebringerova, 2000), consistent with the acid hydrolysis and β-elimination of pectins depolymerization while apple processing (Le Bourvellec et al., 2011). Conversely, two positive peaks at 1595 cm^{-1} and 1030 cm^{-1} could be linked to the increase of lignin (Garside & Wyeth, 2003) and cellulose contents (Fasoli, et al., 2016; □chulz & Baranska, 2007) in cell wall materials. A

368 possible explanation is the depolymerization of cell wall polysaccharides (mainly
369 pectins) during maturation resulting in a relative enrichment of lignin and cellulose in
370 comparison with pectins after apple processing.

371 ATR-FTIR detected the processing changes from raw apples to purees by
372 scanning fresh, freeze-dried and cell wall samples. Particularly, spectra of fresh and
373 freeze-dried samples, i.e. with or without water, provided highly consistent
374 information on internal soluble matters (sugars, acids, pectins and phenolics).
375 Concerning the cell wall depolymerization (mainly pectin solubilization and galactose
376 loss), these change could be detected only by scanning the cell wall materials (AIS),
377 thus highlighting the solubilization of pectins diffusing from pulp to serum (Burgy et
378 al., 2018; □ila et al., 2009).

379 **3.3 Prediction of quality traits: comparison according to sample forms**

380 Acceptable to good predictions of SSC, TA. DMC, fructose and malic acid could
381 be obtained on fresh (NF) and/or freeze-dried (FD) purees by ATR-FTIR, giving RPD
382 from 3.1 to 5.2 (NF) and from 3.6 to 7.6 (FD) **(Table 1)**.

383 The prediction of global fruit quality traits, such as SSC and DMC, depended on
384 two major spectral peaks, respectively, related to the sugars in NF (1061 cm^{-1})
385 (Bureau, Cozzolino, & Clark, 2019) and to the acids in FD (1724 cm^{-1}) (Clark, 2016).
386 In purees, the prediction accuracy of these two quality traits was similar in NF and FD
387 samples with a R_{cv}^2 higher than 0.94 for SSC and higher than 0.89 for DMC. A good
388 correlation between SSC and DMC in purees (R^2=0.78) and the similar related
389 spectral signals used in models (mainly 1724 cm^{-1} and 1061 cm^{-1}) explained the good
390 prediction of both SSC and DMC in NF and FD samples. For the third global quality
391 trait, TA, its prediction was excellent with RPD higher than 6 in NF and FD samples.
392 A particularly strong absorption at 1718 cm^{-1} was used in the TA models in both NF
393 and FD samples.

394 Concerning the main individual sugars and acids (sucrose, fructose and malic
395 acid), ATR-FTIR on FD samples provided more accurate prediction results (R_{cv}^2>0.87
396 and RPD>3.2) than on NF samples (R_{cv}^2>0.79 and RPD>2.3). For fructose and

sucrose, the regression coefficients of the models showed numerous characteristic peaks in the region 1150-900 cm^{-1} in FD samples. But, despite the similar typical peaks, specific peaks such as 1034 cm^{-1} for sucrose and 1084 cm^{-1} for fructose were detected and used in their respective models. The lower RPD and the higher RMSECv in NF than in FD samples were due to the presence of water leading to a lower concentration of components and then a lower sensitivity to their variations. Moreover, to obtain the best prediction of sugars in fresh samples, the spectral region 1700-1550 cm^{-1} specific to soluble substances, was useful. In fresh samples, the linear models for TA, SSC, DMC and malic acid prediction depended foremost on the sugar absorption (fructose and sucrose), because of their relatively higher total concentrations (99.4-228.9 g/kg FW) than those of acids (TA: 25-109.1 meq H^+/kg FW). After freeze-drying, the specific spectral area (1725-1710 cm^{-1}) corresponding to acidity (Clark, 2016) became the main area of PLS models, due to their larger variations during storage than those of individual sugars.

Another quality trait of interest is the AIS contents, which contributes to the rheological properties of the processed apple purees products (Espinosa-Muñoz et al. 2012). The prediction of AIS contents is acceptable with RPD of 3.3 on FD purees, when expressed in dry matter (DW). Its prediction was not possible directly on NF purees. The significant signals at 985 cm^{-1} corresponding to CH stretching of cellulose (Fahey, Nieuwoudt, & Harris, 2017) and at 1147 cm^{-1} for C-O-C vibration of glycosidic bound between uronic acids (Coimbra, Barros, Barros, Rutledge, & Delgadillo, 1998) were in line with the previous PLS models built to predict AIS yield in freeze-dried fruit and vegetables (Canteri, Renard, Le Bourvellec, & Bureau, 2019).

Briefly, ATR-FTIR technique worked well to evaluate global quality traits of interest in apple purees: SSC, TA and DMC. The prediction of cell wall contents (AIS) was possibility only on freeze-dried apple purees. Concerning the detailed composition including the individual components, the prediction was possible directly on fresh puree for malic acid whereas the prediction of the main individual sugars (fructose and sucrose) required the puree freeze-drying. The prediction of glucose was

not acceptable in apple purees whatever the tested conditions.

Surprisingly, prediction was acceptable (R_{cv}^2 >0.87, RPD >3.1) for rheological parameters such as puree viscosity (η_{50} or η_{100}) and visco-elasticity (G', G'' in both amplitude and frequency sweep tests and yield stress) on FD samples with less than 10 LVs and was better than on NF and AIS samples **(Table 2)**. The single shear rate value at 50/s (η_{50}) has been described to be the best correlated with the in-mouth texture perception of fluid foods (Chen & Engelen, 2012). For the two parameters measured at η_{50} and η_{100}, predictions were better in FD samples than in NF and AIS samples. Particularly, two main spectral areas (1718 cm^{-1} and 1620-1595 cm^{-1}) in NF and FD samples appeared to be highly relevant to predict the puree viscosity. Differently, in AIS samples, the two major peaks (1018 cm^{-1} and 1110 cm^{-1}) linked to the viscosity prediction have been conventionally attributed to the pectin changes in fruit cell walls (Coimbra, Barros, Barros, Rutledge, & Delgadillo, 1998). For the specific viscoelastic parameters of purees (AS-G', AS-G'' and yield stress) by amplitude sweep tests, their prediction by ATR-FTIR was excellent in FD samples with RPD values higher than 3.4. The yield stress, corresponding to the moment when the puree starts to flow at the macroscopic level, could be predicted directly on NF purees with the better RPD and RMSECv than on FD samples. From frequency sweep tests (FS), the gel-like behaviors (FS-G' > FS-G'') of all purees could be well estimated in FD samples (R_{cv}^2> 0.90), even with a large variation of FS-G' and FS-G'' **(Table S-3)**. Surprisingly, fresh NF samples were the suitable sample type to evaluate the particle size, both d(4:3) and d(3:2), with a good performance of the PLS models (RPD>3.0).

Although acceptable results of PLS regression were obtained on the three sample types for the prediction of puree rheological properties (viscosity and viscoelasticity) and particle information (sizes and volume), it is worth signaling the differences of their fingerprint peaks: i) for fresh NF samples, the major region between 1750 and 1500 cm^{-1} was attributed to the absorbed water and complex soluble substances (pectins, polyphenols and proteins); ii) for cell wall AI□ extracts, the typical peaks

(1018 cm^{-1}, 1083 cm^{-1}) were mainly related to their pectic and phenolic variations; iii) for freeze-dried FD samples, the specific peaks, 1500-1750 cm^{-1} and 1200-900 cm^{-1}, combining with those observed separately in NF and AIS samples were used. The limited spectral sensitivity for the fresh suspensions (NF) and the restricted variations for the cell wall extracts (AIS) resulted in a less accurate prediction of the rheological behaviors than for freeze-dried FD samples. These results demonstrated the possibility of ATR-FTIR technique to accurately estimate viscosity, elasticity and the particle distributions directly on freeze-dried purees (FD). However, ATR-FTIR on fresh purees (FD) had a good ability to directly evaluate the particle size and properties (RPD>3.0), and also can probably to be used to evaluate the rheological behaviors (viscosity and viscoelasticity) according the results of RPD values over 2.5 (Nicolai et al., 2007).

4. Conclusion

As far as we know, this is the first report concerning the assessment of quality variations in fruit products during processing depending on ATR-FTIR spectral information of the same samples but characterized as fresh, freeze-dried and cell wall extracts. Direct spectral measurements on fresh samples could provide a reliable assessment of texture and major composition characteristics of purees. Thus, ATR-FTIR technique can be adapted to routine analysis in fruit industries, a simple method, using few steps for manufacturers. Long-time freeze-drying preparations still keep the stability and consistency of the ATR-FTIR signals in comparison with those of fresh samples, and provided more detailed assessments of rheological properties and cell wall contents. ATR-FTIR on cell wall materials was the only way to identify the variations of cell wall compositions, but not enough to overview the changes during fruit processing.

Briefly, ATR-FTIR associated with suitable sample pre-treatments in fruit processing could offer sufficient information for the industrial and research demands. Balancing the pre-treated methods to stabilize samples and knowing the potential ability of infrared spectroscopy are both crucial for rapid and accurate analyses in

fruit processing. Based on our results, future works could be extended to a wide span of complex processing strategies (drying, juicing, fermentation etc.) and/or operational units.

Acknowledgements

The authors thank Patrice Reling, Barbara Gouble, Line Touloumet, Marielle Bogé, Caroline Garcia, Gisèle Riqueau and Xuwei Liu (INRAE, SQPOV group) for their technical help. The 'Interfaces' project is an Agropolis Fondation Flashship project publicly funded through the ANR (French Research Agency) under "Investissements d'Avenir" programme (ANR-10-LABX-01-001 Labex Agro, coordinated by Agropolis Fondation). Weijie Lan was supported by a doctoral grant from Chinese Scholarship Council.

References

Abidi, N., Cabrales, L., & Haigler, C. H. (2014). Changes in the cell wall and cellulose content of developing cotton fibers investigated by FTIR spectroscopy. *Carbohydrate Polymers, 100*, 9-16.

Ayvaz, H., Sierra-Cadavid, A., Aykas, D. P., Mulqueeney, B., Sullivan, S., & Rodriguez-Saona, L. E. (2016). Monitoring multicomponent quality traits in tomato juice using portable mid-infrared (MIR) spectroscopy and multivariate analysis. *Food Control, 66*, 79-86.

Baranska, M., Schütze, W., & Schulz, H. (2006). Determination of Lycopene and β-Carotene Content in Tomato Fruits and Related Products: Comparison of FT-Raman, ATR-IR, and NIR Spectroscopy. *Analytical Chemistry, 78*(24), 8456-8461.

Bertrand, D., & Cordella, C. (2008). SAISIR package. Free toolbox for chemometrics in the Matlab, Octave or Scilab environments. In). https://www.chimiometrie.fr/saisir_webpage.html.

Bureau, S., Cozzolino, D., & Clark, C. J. (2019). Contributions of Fourier-transform mid infrared (FT-MIR) spectroscopy to the study of fruit and vegetables: A review. *Postharvest Biology and Technology, 148*, 1-14.

Bureau, S., Quilot-Turion, B., Signoret, V., Renaud, C., Maucourt, M., Bancel, D., & Renard, C. M. G. C. (2013). Determination of the Composition in Sugars and Organic Acids in Peach Using Mid Infrared Spectroscopy: Comparison of Prediction Results According to Data Sets and Different Reference Methods. *Analytical Chemistry, 85*(23), 11312-11318.

Bureau, S., Ruiz, D., Reich, M., Gouble, B., Bertrand, D., Audergon, J. M., & Renard, C. M. G. C. (2009). Application of ATR-FTIR for a rapid and simultaneous determination of sugars and organic acids in apricot fruit. *Food Chemistry, 115*(3), 1133-1140.

Bureau, S., Ścibisz, I., Le Bourvellec, C., & Renard, C. M. G. C. (2012). Effect of Sample Preparation on the Measurement of Sugars, Organic Acids, and Polyphenols in Apple Fruit by Mid-infrared Spectroscopy. *Journal of Agricultural and Food Chemistry, 60*(14), 3551-3563.

Burgy, A., Rolland-Sabaté, A., Leca, A., Le Bourvellec, C., Renard, C. M. G. C. (2018). Molecular size of soluble pectins in apple fruits is not affected by heat processing into puree. *International Conference on Agrophysics Soil, Plant & Climate, Dublin, POL.*

Canteri, M. H. G., Renard, C. M. G. C., Le Bourvellec, C., & Bureau, S. (2019). ATR-FTIR spectroscopy to determine cell wall composition: Application on a large diversity of fruits and vegetables. *Carbohydrate Polymers, 212*, 186-196.

Cardoso, S. M., Mafra, I., Reis, A., Barros, A. S., Nunes, C., Georget, D. M. R., Smith, A. C., Saraiva, J., Waldron, K. W., & Coimbra, M. A. (2009). Traditional and industrial oven-dry processing of olive fruits: influence on textural properties, cell wall polysaccharide composition, and enzymatic activity. *European Food Research and Technology, 229*(3), 415-425.

Clark, C. J. (2016). Fast determination by Fourier-transform infrared spectroscopy of sugar-acid composition of citrus juices for determination of industry maturity standards. *New Zealand journal of crop and horticultural science, 44*(1), 69-82.

Coimbra, M. A., Barros, A., Barros, M., Rutledge, D. N., & Delgadillo, I. (1998). Multivariate analysis of uronic acid and neutral sugars in whole pectic samples by FT-IR spectroscopy. *Carbohydrate Polymers, 37*(3), 241-248.

Colin-Henrion, M., Mehinagic, E., Renard, C. M. G. C., Richomme, P., & Jourjon, F. (2009). From apple to applesauce: Processing effects on dietary fibres and cell wall polysaccharides. *Food Chemistry, 117*(2), 254-260.

de Oliveira, G. A., de Castilhos, F., Renard, C. M. G. C., & Bureau, S. (2014). Comparison of NIR and MIR spectroscopic methods for determination of individual sugars, organic acids and carotenoids in passion fruit. *Food Research International, 60*, 154-162.

Durak, T., & Depciuch, J. (2020). Effect of plant sample preparation and measuring methods on ATR-FTIR spectra results. *Environmental and Experimental Botany, 169*, 103915.

Engelen, L., & de Wijk, R. A. (2012). Oral Processing and Texture Perception. In J. Chen & L. Engelen (Eds.), Food Oral Processing, (pp. 157-176): Wiley-Blackwell.

Espinosa-Muñoz, L., Symoneaux, R., Renard, C. M. G. C., Biau, N., & Cuvelier, G. (2012). The significance of structural properties for the development of innovative apple puree textures. *LWT - Food Science and Technology, 49*(2), 221-228.

Fahey, L. M., Nieuwoudt, M. K., & Harris, P. J. (2017). Predicting the cell-wall compositions of Pinus radiata (radiata pine) wood using ATR and transmission FTIR spectroscopies. *Cellulose, 24*(12), 5275-5293.

Fasoli, M., Dell'Anna, R., Dal Santo, S., Balestrini, R., Sanson, A., Pezzotti, M., Monti, F., & Zenoni, S. (2016). Pectins, Hemicelluloses and Celluloses Show Specific Dynamics in the Internal and External Surfaces of Grape Berry Skin During Ripening. *Plant and Cell Physiology, 57*(6), 1332-1349.

Femenia, A., García-Pascual, P., Simal, S., & Rosselló, C. (2003). Effects of heat treatment and dehydration on bioactive polysaccharide acemannan and cell wall polymers from Aloe barbadensis Miller. *Carbohydrate Polymers, 51*(4), 397-405.

Ferreira, D., Barros, A., Coimbra, M. A., & Delgadillo, I. (2001). Use of FT-IR spectroscopy to follow the effect of processing in cell wall polysaccharide extracts of a sun-dried pear. *Carbohydrate Polymers, 45*(2), 175-182.

Garside, P., & Wyeth, P. (2003). Identification of cellulosic fibres by FTIR spectroscopy-thread and single fibre analysis by attenuated total reflectance. *Studies in conservation, 48*(4), 269-275.

Georget, D. M. R., & Belton, P. S. (2006). Effects of Temperature and Water Content on the Secondary Structure of Wheat Gluten Studied by FTIR Spectroscopy. *Biomacromolecules, 7*(2), 469-475.

Jackson, M., & Mantsch, H. H. (1995). The use and misuse of FTIR spectroscopy in the determination of protein structure. *Critical Reviews in Biochemistry and Molecular Biology, 30*(2), 95-120.

Kacurakova, M., Capek, P., Sasinkova, V., Wellner, N., & Ebringerova, A. (2000). FT-IR study of plant cell wall model compounds: pectic polysaccharides and hemicelluloses. *Carbohydrate Polymers, 43*(2), 195-203.

Kačuráková, M., Wellner, N., Ebringerová, A., Hromádková, Z., Wilson, R. H., & Belton, P. S. (1999). Characterisation of xylan-type polysaccharides and associated cell wall components by FT-IR and FT-Raman spectroscopies. *Food Hydrocolloids, 13*(1), 35-41.

Kyomugasho, C., Christiaens, S., Shpigelman, A., Van Loey, A. M., & Hendrickx, M. E. (2015). FT-IR spectroscopy, a reliable method for routine analysis of the degree of methylesterification of pectin in different fruit-and vegetable-based matrices. *Food Chemistry, 176*, 82-90.

Le Bourvellec, C., Bouzerzour, K., Ginies, C., Regis, S., Plé, Y., & Renard, C. M. G. C. (2011). Phenolic and polysaccharidic composition of applesauce is close to that of apple flesh. *Journal of Food Composition and Analysis, 24*(4-5), 537-547.

Leopold, L. F., Leopold, N., Diehl, H. A., & Socaciu, C. (2011). Quantification of carbohydrates in fruit juices using FTIR spectroscopy and multivariate analysis. *Journal of Spectroscopy, 26*(2), 93-104.

584 Liu, X., Renard, C. M. G. C., Rolland-Sabaté, A., Bureau, S., Le Bourvellec, C. (2019). Modification
585 of cell walls of apple, red beet and kiwifruit by heating in acid conditions: common and
586 specific responses. *15th Cell wall meeting, Cambridge, UK.*
587 Lu, X., Wang, J., Al-Qadiri, H. M., Ross, C. F., Powers, J. R., Tang, J., & Rasco, B. A. (2011).
588 Determination of total phenolic content and antioxidant capacity of onion (Allium cepa) and
589 shallot (Allium oschaninii) using infrared spectroscopy. *Food Chemistry, 129*(2), 637-644.
590 Nargis, H., Nawaz, H., Ditta, A., Mahmood, T., Majeed, M., Rashid, N., Muddassar, M., Bhatti, H.,
591 Saleem, M., & Jilani, K. (2019). Raman spectroscopy of blood plasma samples from breast
592 cancer patients at different stages. *Spectrochimica Acta Part A: Molecular and Biomolecular*
593 *Spectroscopy, 222*, 117210.
594 Nicolai, B. M., Beullens, K., Bobelyn, E., Peirs, A., Saeys, W., Theron, K. I., & Lammertyn, J. (2007).
595 Nondestructive measurement of fruit and vegetable quality by means of NIR spectroscopy: A
596 review. *Postharvest Biology and Technology, 46*(2), 99-118.
597 Oliveira-Folador, G., de Oliveira Bicudo, M., de Andrade, E. F., Renard, C. M. G. C., Bureau, S., & de
598 Castilhos, F. (2018). Quality traits prediction of the passion fruit pulp using NIR and MIR
599 spectroscopy. *LWT - Food Science and Technology, 95,* 172-178.
600 Rawle, A. (2003). Basic of principles of particle-size analysis. *Surface coatings international. Part A,*
601 *Coatings journal, 86*(2), 58-65.
602 Renard, C. M. G. C. (2005). Variability in cell wall preparations: quantification and comparison of
603 common methods. *Carbohydrate Polymers, 60*(4), 515-522.
604 Schulz, H., & Baranska, M. (2007). Identification and quantification of valuable plant substances by IR
605 and Raman spectroscopy. *Vibrational Spectroscopy, 43*(1), 13-25.
606 Sila, D., Van Buggenhout, S., Duvetter, T., Fraeye, I., De Roeck, A., Van Loey, A., & Hendrickx, M.
607 (2009). Pectins in processed fruits and vegetables: Part II Structure function relationships.
608 *Comprehensive reviews in food science and food safety, 8*(2), 86-104.
609 Soukup, A. (2014). Selected Simple Methods of Plant Cell Wall Histochemistry and Staining for Light
610 Microscopy. In V. Žárský & F. Cvrčková (Eds.), *Plant Cell Morphogenesis: Methods and*
611 *Protocols*, (pp. 25-40). Totowa, NJ: Humana Press.
612 Szymanska-Chargot, M., Chylinska, M., Kruk, B., & Zdunek, A. (2015). Combining FT-IR
613 spectroscopy and multivariate analysis for qualitative and quantitative analysis of the cell wall
614 composition changes during apples development. *Carbohydrate Polymers, 115*, 93-103.
615 U.S. Department of Agriculture, Agricultural Research Service. (2019) Apples, raw, with skin (Includes
616 foods for USDA's Food Distribution Program). Uploaded on January 4, 2019, from
617 https://fdc.nal.usda.gov/ fdc-app.html#/food-details/171688/nutrients
618 Van Boekel, M. A. J. S. (2008). Kinetic Modeling of Food Quality: A Critical Review. *Comprehensive*
619 *reviews in food science and food safety, 7*(1), 144-158.
620 Varela, P., Salvador, A., & Fiszman, S. (2007). Changes in apple tissue with storage time: Rheological,
621 textural and microstructural analyses. *Journal of Food Engineering, 78*(2), 622-629.
622

623 **Figure captions**

624 **Figure 1.** Experimental scheme for apple and puree samples preparation,
625 characterization using ATR-FTIR and reference analyses.

626 **Figure 2.** PCA on the SNV pre-treated ATR-FTIR spectra (900-1800 cm^{-1})of purees
627 (NF samples) prepared with normal thinned 'Granny Smith' apples (GS marked with
628 △), thinned (Th+) 'Golden Delicious' apples (GD Th+ marked with ○) and
629 non-thinned 'Golden Delicious' apples (GD Th- marked with □) stored in cold
630 storage room (4°C) during 0, 1, 3 and 6 months (T0, T1, T3 and T6): (a) the scores
631 plot of the two first components (PC1 and PC2); (b) the loading plot of PC1; (c) the
632 loading plot of PC2.

633 **Figure 3.** FDA on the SNV pre-treated ATR-FTIR spectra (900-1800 cm^{-1}) of
634 non-refined (* with 95% confidence ellipse circles) and refined (△ with 95%
635 confidence ellipse circles) 'Golden Delicious' and 'Granny Smith' purees at harvest
636 (T0), after one-month (T1), three months (T3) and six months (T6) of storage at 4°C.
637 Macroscopic laser scanning images of puree particle distributions at harvest (T0) and
638 after six-month storage (T6).

639 **Figure 4.** Maps of Factorial Discriminant Analysis (FDA) performed on the
640 SNV-pre-treated ATR-FTIR spectra (900-1800 cm^{-1}) of all fresh apple homogenates
641 (named 'Ho') and the corresponding processed purees (named 'Pu') with: (a) fresh
642 samples ('NF'), (c) freeze-dried samples ('FD'), (e) cell wall samples ('AIS'); (b) the
643 second factorial score ('F2') of fresh samples, (d) the second factorial score ('F2') of
644 freeze-dried samples ('FD'); (f) the first factorial score ('F1') of cell wall samples.

Figures

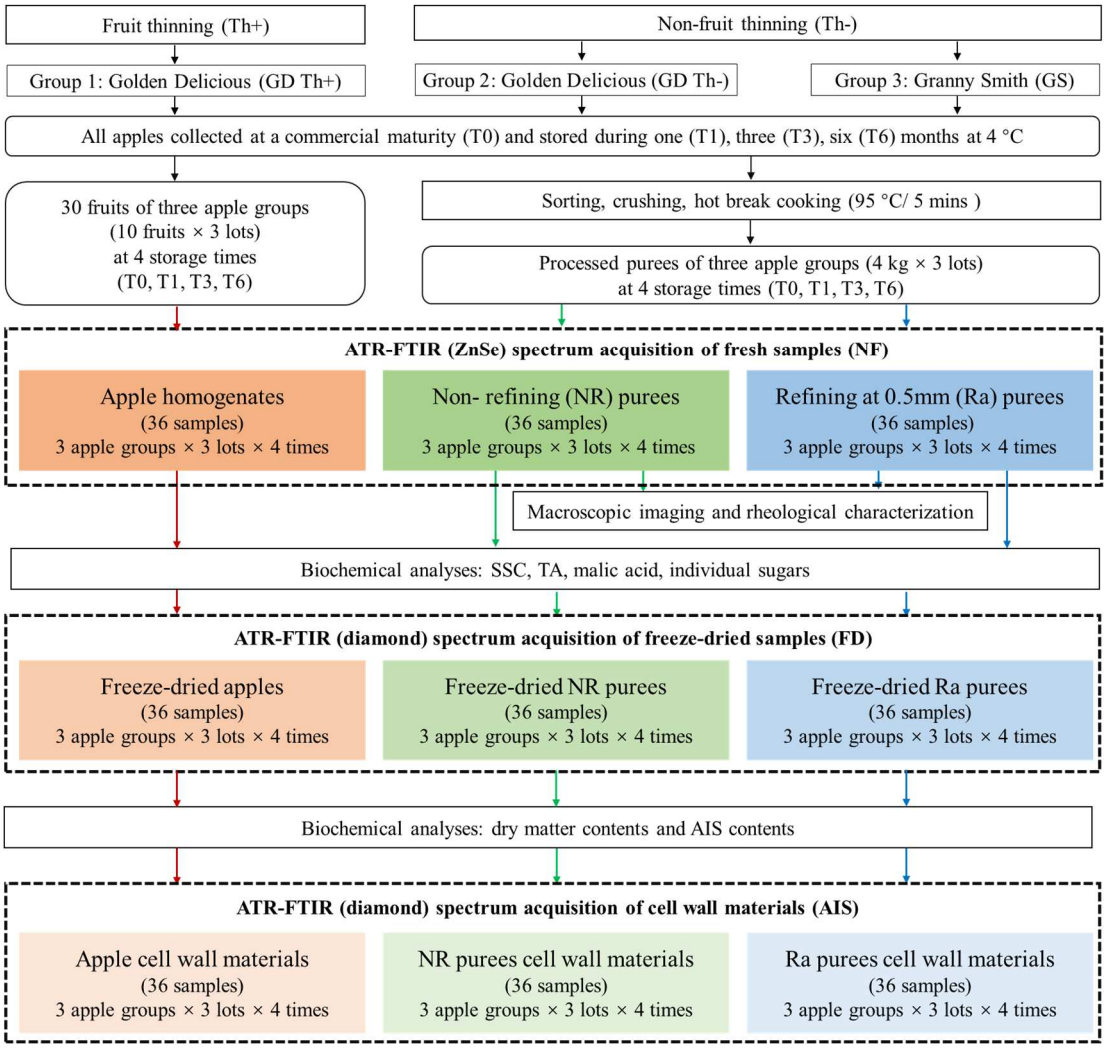

Figure 1

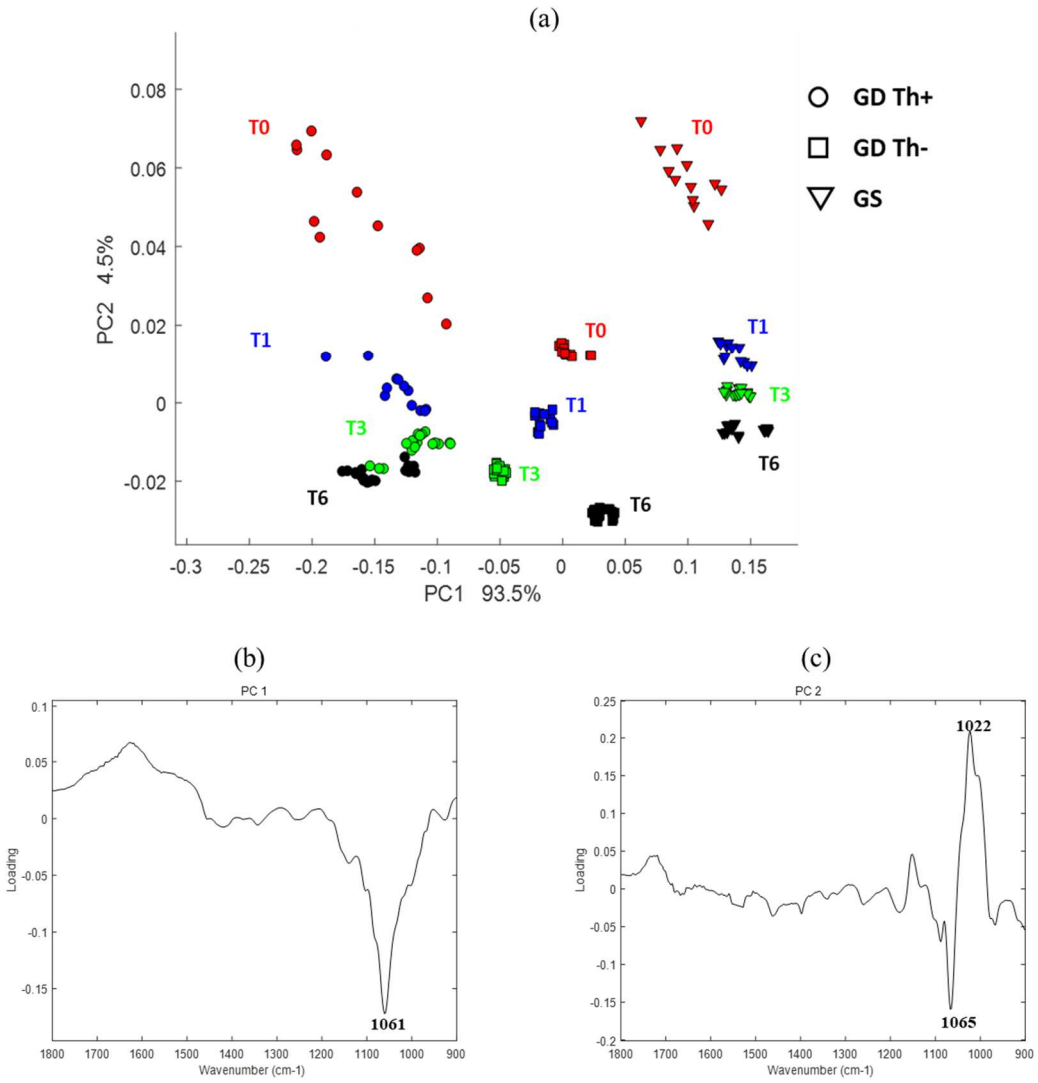
(a)
GD Th+
GD Th-
GS
PC2 4.5%
PC1 93.5%
T0
T1
T3
T6
(b)
PC 1
Loading
Wavenumber (cm-1)
1061
(c)
PC 2
Loading
Wavenumber (cm-1)
1022
1065

Figure 2

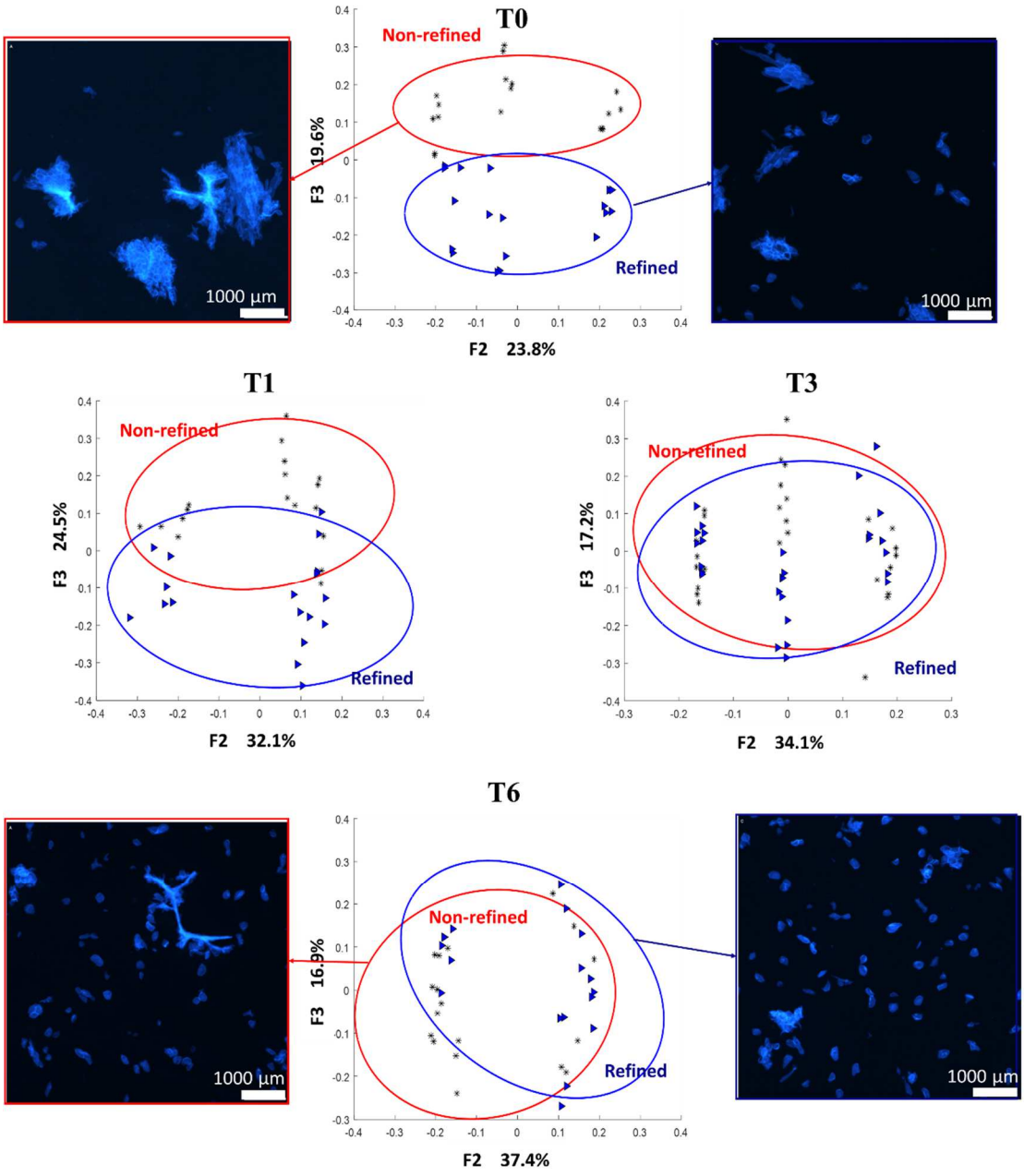

651

652 **Figure 3**

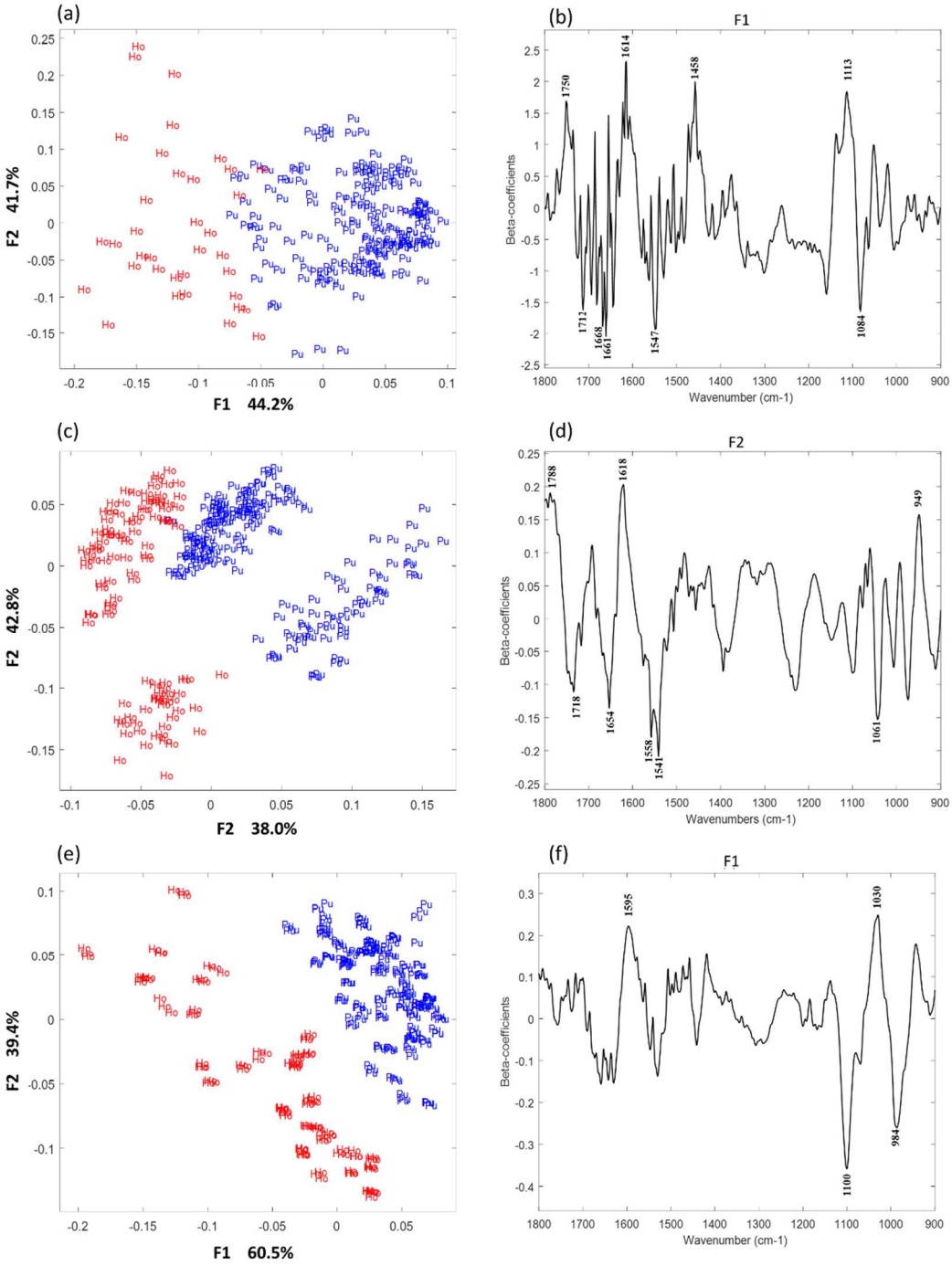
(a)
F2 41.7%
F1 44.2%
(b)
F1
Beta-coefficients
Wavenumber (cm-1)
1750
1614
1458
1113
1712
1668
1661
1547
1084
(c)
F2 42.8%
F2 38.0%
(d)
F2
Beta-coefficients
Wavenumbers (cm-1)
1788
1618
949
1718
1654
1558
1541
1061
(e)
F2 39.4%
F1 60.5%
(f)
F1
Beta-coefficients
Wavenumber (cm-1)
1595
1030
1100
984

Figure 4

Table 1. Prediction of apple processed purees composition using the leave-one-out PLS regression based on the fresh ('NF') and freeze-dried ('FD') ATR-FTIR spectra and reference data.

				Leave-one-out PLS (n=72)				
Parameter	Sample	Range	SD	R_{cv}^2	RMSECv	LVs	RPD	Linkable regions (cm^{-1})
SSC (°Brix)	NF	10.3-18.6	2.4	0.94	0.6	4	4.1	1055-1065, 1028-1030, 1558-1562, 1649-1653
	FD			0.95	0.5	3	4.9	1058-1065, 1724-1735, 998-1001
Sucrose (g/kg FW)	NF	32.2-123.1	24.2	0.79	10.5	8	2.3	1084-1095, 1030-1034, 1574- 1583, 1225-1229, 916-920, 998-1102
	FD			0.87	7.8	7	3.2	998-1001, 1080-1084, 1030-1034, 1124-1137, 998-1102
Glucose (g/kg FW)	NF	13.5-25.7	3.4	0.65	2.0	9	1.7	1720-1715, 1656-1645, 1539-1562, 1886-1753, 1163, 1067, 1015
	FD			0.70	1.8	6	1.9	1028-1034, 1578-1570, 1010-1015, 1420- 1397, 1079, 985-998
Fructose (g/kg FW)	NF	40.0-99.9	18.9	0.88	6.0	8	3.1	1635-1655, 1078-1086, 1028-1034, 987-998, 1137-1142
	FD			0.90	5.3	6	3.6	1082-1090, 1030-1034, 987-989, 926-928, 1061-1665, 1035-1046
TA (meq/kg FW)	NF	25.0-109.1	22.8	0.97	3.8	4	6.0	985-998, 1084-1095, 1715-1730, 1695-1701
	FD			0.98	3.0	3	7.6	1716-1724, 987-989, 962-968
Malic acid (g/kg FW)	NF	2.35-8.97	1.63	0.91	0.5	4	3.3	1082-1095, 995-1001, 1715-1730, 1539
	FD			0.94	0.4	5	4.3	1716-1733, 1541-1558, 1695-1705, 1022-1024
DMC (g/g FW)	NF	0.16-0.24	0.03	0.89	0.01	6	3.1	1055-1068, 1443-1430, 1113-1135, 965-978, 1741-1730
	FD			0.92	0.01	5	3.6	1710-1728, 1541-1558, 1514-1507
AIS content (mg/g DW)	NF	100.4-271.7	33.3	0.75	16.9	10	1.9	1665-1685, 1701-1718, 1113-1128, 962-968, 1548-1560, 1605-1620
	FD			0.88	10.1	7	3.3	1142-1150, 985-995, 1058-1065, 1058, 995-1005, 1650-1665
AIS content (mg/g FW)	NF	16.5-48.9	6.1	0.76	3.5	9	2.0	1655-1685, 1605-1620, 1665-1685, 1700-1722, 965-985, 1094-1105
	FD			0.83	2.3	8	2.7	1055-1065, 985-995, 1030-1035, 1142-1150, 1165-1193, 1096-1101

Puree spectra and reference data from two varieties ('Granny Smith', 'Golden Delicious') with different thinning conditions, a cold storage (during 0, 1, 3 and 6 months) and two puree refining conditions. Spectral area: 1800-900 cm^{-1} and spectrum pre-processing: baseline-correction and SNV.

Table 2 Prediction of apple processed purees rheological parameters and textural properties using the leave-one-out PLS regression based on the fresh (NF), freeze-dried (FD) and cell wall (AIS) ATR-FTIR spectra and reference data.

				Samples (n=72)				
Parameter	Sample	Range	SD	R_{cv}^2	$RMSEC_V$	LVs	RPD	Linkable regions (cm^{-1})
η50	NF	0.69-1.94	0.44	0.84	0.18	8	2.5	1620-1635, 1662-1670, 1718-1726, 1110-1122, 1080-1109, 1450-1456
	FD			0.88	0.14	9	3.1	940-952, 1060-1065, 1455-1471, 925-935, 1078-1084, 1145-1150, 1718-1726
	AIS			0.86	0.16	8	2.8	1018-1023, 1110-1115, 1160-1168, 1057-1083, 925- 935, 1618-1625
η100	NF	0.25-1.06	0.21	0.83	0.09	8	2.5	1610-1620, 1718-1726, 1560-1584, 1080-1110, 1450-1456
	FD			0.89	0.06	9	3.4	940-952, 1060-1065, 1150-1161, 1455-1471, 1020-1038, 983-995,
	AIS			0.84	0.08	9	2.6	1018-1023, 1092-1110, 924- 935, 1057-1083, 1610-1625, 946-958
AS-G' (Pa)	NF	6-3612	1001	0.82	425	10	2.4	1645-1665, 1047-1055, 1082-1088, 1450-1456, 1530-1547, 925-932,
	FD			0.88	297	9	3.4	1020-1036, 1618-1635, 1060-1065, 1455-1471, 1084-1090, 983-995
	AIS			0.85	332	9	3.0	1610-1625, 1078-1113, 1018-1023, 924- 935, 1039-1043, 1193-1216
AS-G'' (Pa)	NF	2-860	234	0.83	98	9	2.5	1530-1547, 1456-1464, 1645-1665, 1080-1088, 1610-1618, 925-932
	FD			0.89	69	10	3.4	1015-1030, 1060-1068, 930-944, 1084-1090, 1465-1482, 1624-1643
	AIS			0.86	72	9	3.1	1018-1023, 1078-1110, 1560-1584, 1610-1625, 924-935, 1193-1216
yield stress	NF	0.6-57.6	12.9	0.86	4.4	9	2.9	1082-1088, 1530-1547, 1686-1699, 1030-1043, 1610-1618, 1090-1111,
	FD			0.87	4.2	9	3.1	984-992, 1463-1470, 1048-1054, 935-944, 1142-1151, 1465-1482, 1090-1104
	AIS			0.82	4.9	9	2.6	1039-1056, 1018-1023, 1078-1110, 946-958, 924- 935, 1610-1625
FS-G' (Pa)	NF	0.3-3105.6	798.2	0.84	303.5	8	2.6	1645-1665, 1530-1549, 1456-1464, 1610-1620, 1058-1063
	FD			0.90	217.6	10	3.3	946-955, 1015-1030, 1455-1471, 1090-1104, 1060-1068, 1612-1620
	AIS			0.84	292.4	8	2.5	1018-1023, 1610-1625, 1092- 1110, 912-930, 1039-1056
FS-G'' (Pa)	NF	0.3-511.1	158.7	0.82	63.3	10	2.5	1645-1665, 1456-1464, 1530-1549, 1685-1695, 1058-1063, 1610-1618,
	FD			0.91	48.1	8	3.3	937-949, 1060-1068, 1455-1471, 1011-1028, 1455-1462, 1092-1104
	AIS			0.87	56.1	10	2.9	1018-1023, 1570-1584, 1528-1542, 1092-1110, 1610-1625, 912-924

	NF			0.90	59	9	3.3	1701-1710, 1655-1668, 1034-1038, 1718-1726, 986-995, 1534-1541,1145-1152
d (4:3)	FD	277-920	195	0.93	53	9	3.5	934-949, 1464-1482, 1540-1558, 1050-1056, 915-920, 1740-1765
	AIS			0.87	65	8	3.0	1045-1083, 1502-1516, 1059-1067, 956-980, 1605-1615
	NF			0.86	21	10	3.0	1146-1158, 1034-1038, 1405-1412, 1082-1119, 1560-1597, 986-995, 1730-1742
d (3:2)	FD	132-422	64	0.85	23	10	2.8	1027-1039, 1056-1065, 1110-1124, 915-939, 1008-1015, 1625-1648
	AIS			0.81	26	9	2.3	974-995, 1018-1023, 1235-1256, 1045-1083, 1727-1735, 1605-1615

Puree spectra and reference data from two varieties ('Granny Smith', 'Golden Delicious') with different thinning conditions, a cold storage (during 0, 1, 3 and 6 months) and two puree refining conditions. Spectral area: 1800-900 cm^{-1} and spectrum pre-processing: baseline-correction and SNV.